

# INTERNATIONAL SOCIETY FOR SOIL MECHANICS AND GEOTECHNICAL ENGINEERING



*This paper was downloaded from the Online Library of the International Society for Soil Mechanics and Geotechnical Engineering (ISSMGE). The library is available here:*

<https://www.issmge.org/publications/online-library>

*This is an open-access database that archives thousands of papers published under the Auspices of the ISSMGE and maintained by the Innovation and Development Committee of ISSMGE.*

*The paper was published in the Proceedings of the 8<sup>th</sup> International Symposium on Deformation Characteristics of Geomaterials (IS-PORTO 2023) and was edited by António Viana da Fonseca and Cristiana Ferreira. The symposium was held from the 3<sup>rd</sup> to the 6<sup>th</sup> of September 2023 in Porto, Portugal.*

# Soft-rigid granular mixtures: role of particle shape and rolling resistance in response under compressive loads

Mehdi Alam<sup>1,2</sup>, Arghya Das<sup>1</sup>, and Mahdi M. Disfani<sup>2#</sup>

<sup>1</sup>Indian Institute of Technology, Kanpur Department of Civil Engineering, Kanpur, Uttar Pradesh, India

<sup>2</sup>The University of Melbourne, Department of Infrastructure Engineering, Melbourne, Australia

<sup>#</sup>Corresponding author: mmiri@unimelb.edu.au

## ABSTRACT

Mixtures of recycled tyre aggregates and common granular geo-material such as gravel and sand have been widely used for various applications in geotechnical engineering, such as backfill, lightweight construction geomaterial and pavement subbase layers. The mechanical properties and characteristics of various soft-rigid granular blends has been extensively studied in the past. The main objective of these studies is to determine suitable mix designs for different applications and provide a better understanding of material response under applied loads. Experimental and numerical studies indicate the paramount importance of particle interaction at the microscale on the response of the soft-rigid granular mixtures at the macro scale. The stark contrast in stiffness (or flexibility) of soft tyre particles to rigid sand or gravel particles, means that in the soft-rigid mixtures under shearing or compressive loads, the deformation of soft tyre particles and continuous change of shape and contact area and hence constant evolution of frictional resistance plays an important role in the behaviour of these blends. In the present research mixtures of gravel and tyre particles in a range of volume ratios and size ratios were modelled using DEM (discrete element method) and calibrated to match one-dimensional compressibility experimental data obtained by the team. The effect of the shape of soft particles on the compressive response of soft-rigid granular mixtures is studied through rolling resistance in DEM. The role of rolling friction is studied in detail. Rolling resistance is found to be an important parameter to simulate the behaviour of the particle shape of these mixtures. Microscopic studies like spin analysis and share of contact force is performed to understand the observed response better. However, the increase in rolling resistance value beyond a calibrated value is found to have little impact on the macroscopic behaviour of these mixes.

**Keywords:** Recycled tyre aggregates; Soft-rigid granular mixtures; Rolling resistance; Discrete element modelling.

## 1. Introduction

Soft-rigid granular mixtures such as tyre aggregates and gravel or sand is a viable solution to replace the conventional granular mixes such as sand and gravel. Further uptake on soft-rigid granular mixes can help in reducing the use of regular geomaterials and enhance the use of waste materials such as waste tyre aggregates which can ultimately help to curb environmental pollution. Several researchers in the past have studied these mixes using experimental and numerical techniques to determine optimum mix design corresponding to required strength and stiffness at the micro and macro levels (Lee et al., 2009; Lee et al., 1999; Liu et al., 2020; Lopera et al., 2016; Wang et al., 2018; Fonseca et al., 2019). In the optimum mix, size and shape of soft tyre particles play a crucial role in controlling the mechanical properties of the mixture. For instance, (Lee et al., 2007) and (Kim & Santamarina, 2008) used soft particles of size 1/4th and 10 times of the rigid particles, respectively. The results indicate that the strength and stiffness of the mixture decreases with increasing the volume of the soft particles in the mix. However, segregation is found to be a major concern with higher percentage of soft particle addition. In order to reduce the repetitive experimental effort in determining the mix design performance, Discrete Element Modelling is used to provide DEM

based microstructural analysis as a viable alternative. Use of DEM in studying soft-rigid granular mixture has been quite common given the particulate nature of the soft-rigid granular mixtures and the ability of DEM to provide information at particulate level. Asadi et al., 2018a; Asadi et al., 2018b performed a series of experiments and DEM simulations replicating these mixes to capture the particle-scale response of material. Microscopic analysis using DEM is challenging due to the soft nature of tyre particles and evolving shape caused by compression. A few studies considered generating realistic tyre particles' shape in DEM, while majority of the studies assumed idealized spherical particles. Introducing advanced contact law such as rolling resistance can overcome shape related issues associated to soft-rigid mixture simulation in DEM. Liu et al., 2020 performed true triaxial test using DEM using rolling resistance linear contact model. The present study provides a detailed analysis on the efficacy of rolling friction as a proxy to soft particle shape in DEM for particulate study of soft-rigid granular mixtures.

## 2. Experimental Investigation

In the present study, experimental analysis by Raessi et al. (2021) from our research team on the mechanical behaviour of crushed rock (CR) mixed with tyre-derived rubber granulates is used for the calibration purpose. 1D compression or oedometer experiments were conducted

with four different soft (rubber) volume fractions (0%, 20%, 40% and 60%) against the rigid particles. The samples are prepared in an oedometer ring having 50 mm diameter and 25 mm height (Fig. 1). In the experiments, the behaviour of the mixes is quantified in terms of constrained modulus and void ratio evolution against the applied vertical stress for different percentages of soft and different percentages of binder content (for the bonded soft-rigid granular mixtures). However, for the present analysis, the response of the unbonded mix is used.

In addition to the mechanical responses of the mix, the morphological changes in soft rubber particles during 1D compression are qualitatively analysed through image processing using X-ray tomography. In the present study, the mixture with 60% soft by volume is chosen to better understand the behaviour of the soft particles in the mixture. Four strain levels (0%, 8%, 14% and 20%) are applied to the sample. Subsequent distances between the top and bottom cap of the ring are calculated at each strain level using vernier calipers, as shown in Fig. 1. At each strain level the sample is mounted at the compression chamber, and an X-ray source with energy of 140kV and 300  $\mu$ A with 0.1mm copper (Cu) filter to pre-harden the X-ray is used to obtain images of sample. X-ray scans are taken at a resolution of 25 $\mu$ m. Median filter, region of interest (ROI) filter and beam hardening correction are applied during image reconstruction.

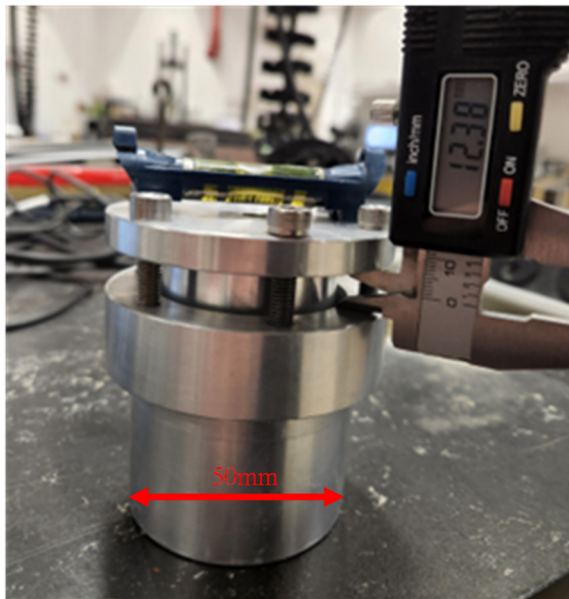


**Figure 1.** Experimental setup with strain measurement procedure for initial sample

The CT scan images are then sliced to obtain the vertical slices at each strain level. A watershed algorithm is applied to separate the different phases from the original images. This method has proven to be useful to separate different phases of granular media (Ahmadi et al., 2021). The segmented results can be seen in Fig. 2 with increasing strain levels. Here, the soft particle is represented by black, rigid particles are white, and the remaining grey zones are void spaces. It is evident from the images that the soft particles tend to deform under compressive loading considerably, and hence major

shape changes occur for these particles. This morphological evolution leads to a change in contact properties between the soft-soft and soft-rigid contacts.

In numerical modelling with DEM, the current study attempts to model the particle shape and its evolution during compression using rolling resistance, which is discussed in the subsequent sections.

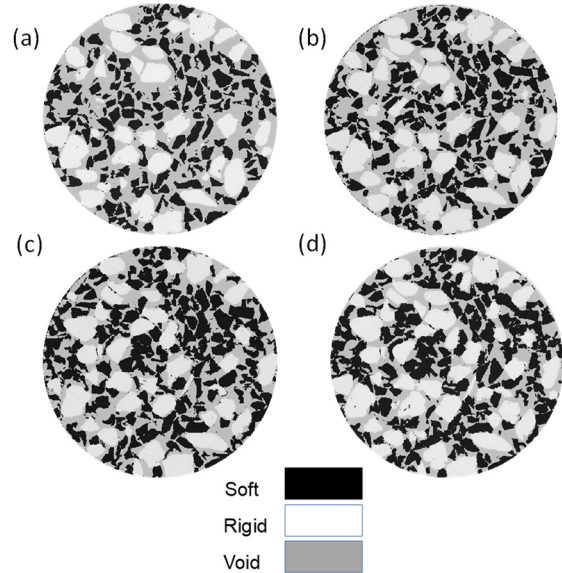


**Figure 2.** Segmented CT-scan images at different strain levels (a) 0% (b) 8% (c) 14% (d) 20%.

### 3. DEM Analysis

This study uses PFC 3D (6.0) (PFC | US Minneapolis - Itasca Consulting Group, Inc.) to model the behaviour of soft-rigid mixes. Oedometric compression tests are simulated by placing the mixtures within a rigid cylindrical container of diameter 0.105 m and 0.05 m height, similar to the experimental work. The container is enclosed with two flat platens. During the compression, both platens are moved with a constant velocity of 0.01 m/s. The velocity is attained gradually to avoid an abrupt change in the stress-strain response. The rolling resistance contact model is used in the current study to simulate the behaviour of the soft-rigid mixes. The contact parameters are obtained from the experimental analysis by Raessi et al. (2021). Two different mixtures (0% and 20% soft particle by volume) are initially modelled to determine different contact parameters. This is because these contacts are significantly fewer than the other contacts in mixtures with low soft particle content and hence have a lower impact on the overall stress-strain response. In the later part of the study, samples with a higher percentage of soft particles (40% and 60%) are used for contact analysis.

#### 3.1 Rolling resistance linear contact model

The rolling resistance linear contact model is used in the current study. Various researchers (Gong et al., 2019; Liu et al., 2020) have used this model in the past due to its ability to replicate the shape effect of the particles to a certain extent. Also, this approach is computationally efficient compared to models that generate real particle shapes ((Asadi et al., 2018). Four different types of

contact are considered for the present study, namely soft-soft, rigid-rigid, soft-rigid and wall-particle. It should also be noted that separate contact properties are not assigned for soft-wall and rigid-wall contacts (Liu et al., 2020).

A schematic representation of the rolling resistance linear model is shown in Fig. 3. More details on the linear contact model, are provided in Cundall & St (1979).

The rolling resistance contact model updates the force and moment according to Eq. (1).

$$F_c = F^l + F^d, M_c = M^r \quad (1)$$

where  $F^l$  is the linear and  $F^d$  is the dashpot forces.  $M^r$  represents the rolling resistance moment and is incremented as Eq. (2) if the calculated value is less than the limiting torque which is obtained from Eq. (3), otherwise limiting torque is considered for rolling resistance moment calculation.

$$M^r := M^r - k_r \Delta \theta_b \quad (2)$$

$$M^* = \mu_r R F_n^l \quad (3)$$

$\Delta \theta_b$  is the relative bend-rotation increment,  $R$  is the effective contact radius,  $F_n^l$  is the linear contact normal force and  $k_r$  is the rolling stiffness which is calculated as presented in Eq. (4).

$$k_r = k_s R^2 \quad (4)$$

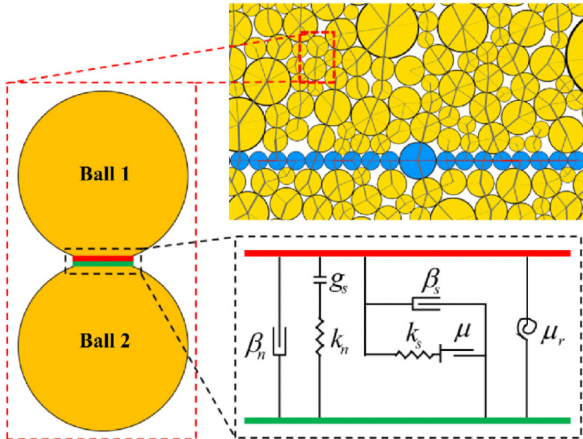


**Figure 3.** Schematic diagrams of rolling resistance linear model.  $k_n$  and  $k_s$  are the normal and shear stiffness of the linear spring, respectively;  $\beta_n$  and  $\beta_s$  are the normal and shear dashpots, respectively;  $g_s$  is the surface gap (non-tension joint);  $\mu$  is the friction coefficient;  $\mu_r$  is the rolling resistance coefficient (Ma et al., 2020)

### 3.2 Contact parameter calibration

#### 3.2.1 Particle size distribution (PSD)

The sample is prepared with spherical particles with the same particle size distribution (PSD) as the experimental work of Raeesi et al., (2021). The samples are prepared using 0%, 20% (Fig. 4(a).), 40% and 60% by volume of soft particles. Particles are generated using the ball-distribute feature of PFC in two groups, soft and rigid particles. The final PSD of the assembly generated in PFC for this study can be seen in Fig. 4(b).

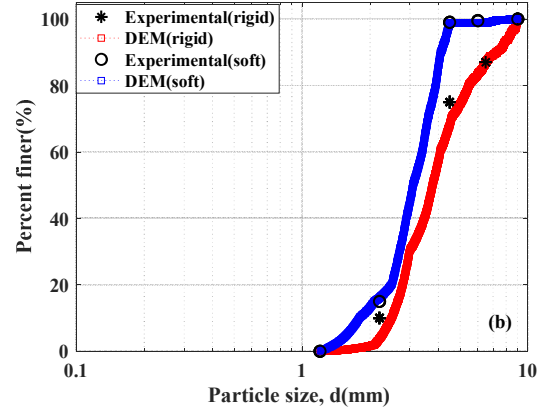
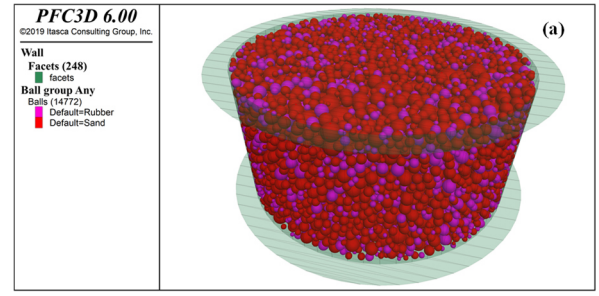
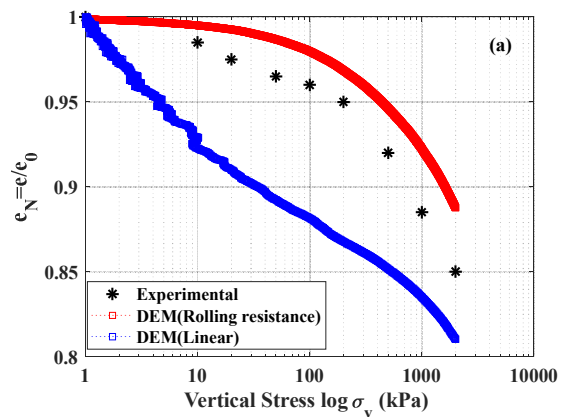


**Figure 4.** (a) Sample prepared in PFC3D 6.00 (20% soft particles content) (b) PSD calibration for soft and rigid particles.

#### 3.2.2 Rigid-rigid contact parameters

A trial-and-error approach is adopted to calibrate all the contact parameters (linear stiffness, rolling resistance, frictional resistance). Initially, a sample with only the rigid particles is prepared to calibrate the rigid-rigid contact parameters (Fig. 5(a)). The evolution of macroscopic constrained modulus and void ratio against the axial stress response of experimental 1D compression tests (Raeesi et al., 2021) is compared with the DEM predictions for the parameter calibration. The soft-soft and soft-rigid contact parameters are calibrated using a 20% soft particle sample. Raeesi et al. (2021) introduced a corrected void ratio definition for soft-rigid mixture sample preparation in DEM.

The parameters that provide the best-fit response are listed in Table 1.



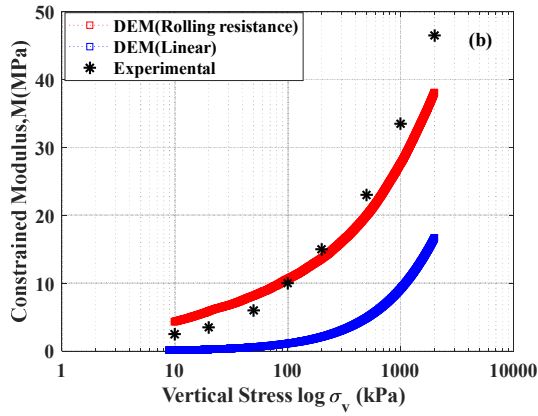


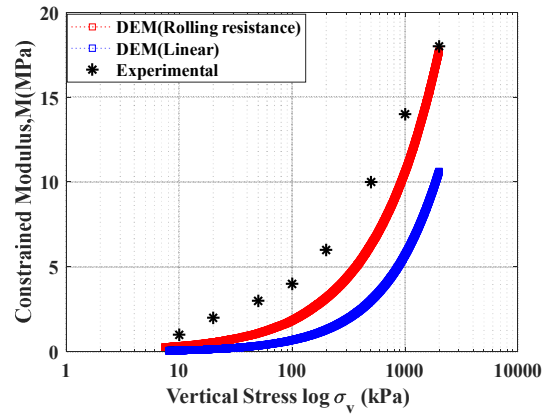
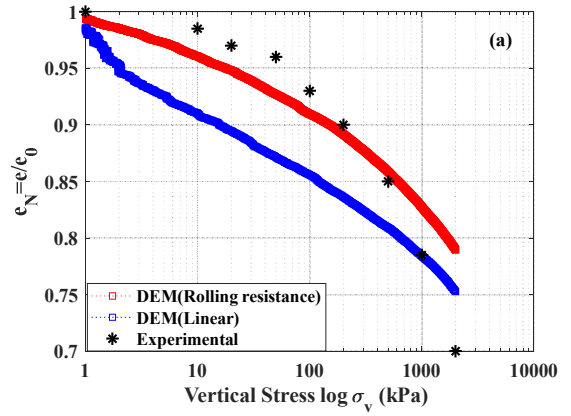
**Figure 5.** Calibration of rigid-rigid contact parameters (a) Void ratio (b) Constrained Modulus for 0% soft content sample.

**Table 1.** Calibrated contact parameters

Type of contact		Rigid-Rigid	Soft-Soft	Rigid-Soft	Particle-wall
Linear Group	Coefficient of friction ( $\mu$ )	0.6	0.8	0.5	0
	Effective modulus ( $E^*$ , N/m <sup>2</sup> )	$5 \times 10^8$	$5 \times 10^6$	$5 \times 10^8$	$5 \times 10^8$
	Normal to shear stiffness ratio ( $k_n/k_s$ )	1	1	1	1
Dashpot Group	Normal critical damping ratio ( $\beta_n$ )	0.7	0.7	0.7	--
	Shear critical damping ratio ( $\beta_s$ )	0.7	0.7	0.7	--
Rolling resistance group	Rolling friction coefficient ( $\mu_r$ )	0.35	1	0.8	--

### 3.2.3 Rigid-soft contact parameters

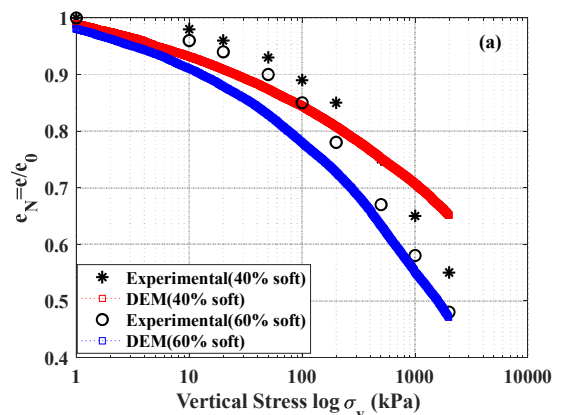
The comparison of numerical and experimental results is given in Fig. 6, which shows a good agreement between experimental work and DEM.



**Figure 6.** Calibration of rigid-soft and soft-soft contact parameters using 20% soft content (a) Void ratio (b) Constrained Modulus.

A similar procedure adopted for the rigid sample is used for the calibrated contact parameters listed in Table 1.

It should be noted that the soft-soft contact stiffness is significantly lower than the rigid particle contact. All these contact parameters are used to validate the results for granular assemblies with 40% and 60% by volume of soft particles in a soft-rigid mix (Fig. 7). However, unlike the samples with 0% and 20% soft particle content, the response of sample with 40% and 60% soft particle content only qualitatively agrees with the experimental response as can be observed in Fig. 7. Such deviation may be attributed due to the nonlinear contact stiffness which is not accounted for in the present analysis.



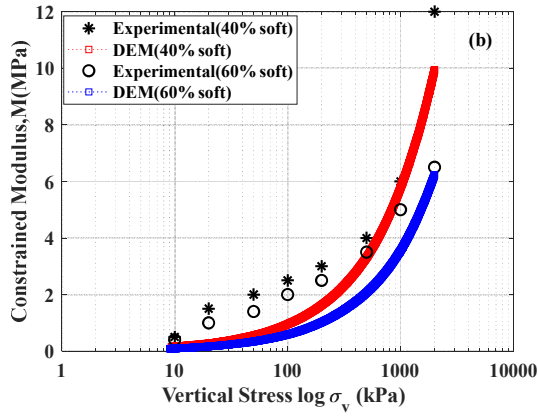


Figure 7. Response for 40% and 60% soft particle content mixtures (a) Void Ratio (b) Constrained Modulus.

### 3.3 Impact of rolling resistance

In the present study rolling resistance effect as a proxy to particle shape is analysed in two ways, constant initial rolling resistance for soft particles as part of calibration process, and a gradually evolving rolling resistance to mimic shape change in soft particles with increasing compression. Fig. 5 and 6 compare two possible cases of rolling friction for different samples, a finite/calibrated rolling friction and zero rolling friction case. The results highlight that rolling resistance has an immense influence on the response on the soft-rigid mixture. A linear contact model with no restraint in the particle rotation distinctly underestimates the stiffness of the granular mixture.

Fig. 8 demonstrates two rolling friction cases for soft particle contacts in 60% soft particle specimen. However, any further increase in rolling resistance beyond the calibrated values has little influence on the macroscopic response of the sample. Further, normal contact force share among rigid-rigid, rigid-soft and soft-soft contacts are compared for a wide range of rolling friction, starting from 0.3 to 2.5 for the soft particles. Fig. 9 indicates that for a sample with 60% soft particles, the contact force share is unaffected by increasing rolling resistance. An additional numerical study with a varying rolling resistance is performed to better understand the importance of rolling resistance in replicating the evolution of soft particle shape. In this process, rolling resistance is gradually reduced as the compression progresses for the soft particles. This simulation is performed to understand if the effect of shape change for soft particles during the reduction can be taken care by changing rolling resistance alone.

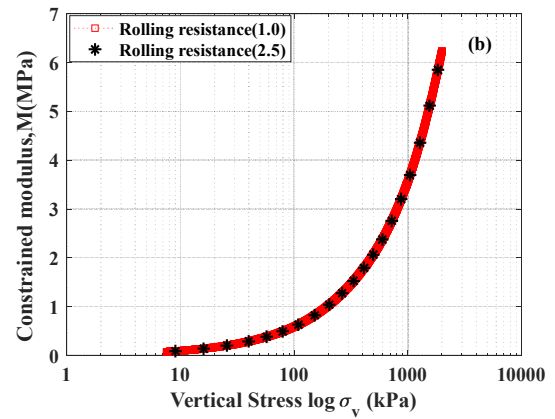
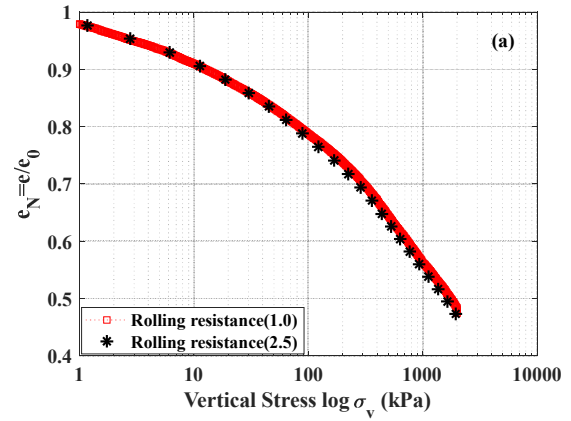


Figure 8. Response of 60% soft particles content mixtures for two different rolling resistance (a) void ratio (b) Constrained Modulus.

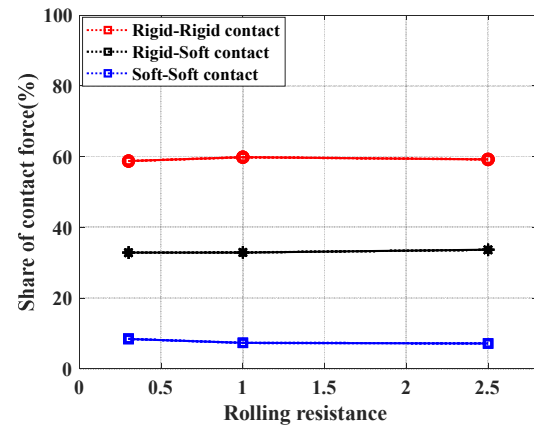
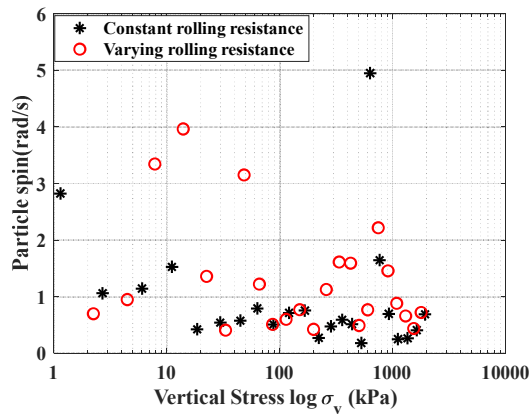


Figure 9. Contact force share with different rolling resistance for sample with 60% soft particles.

### 3.4 Particle rotation analysis

Particle rotation (spin) is captured during compression for the constant and varying rolling resistance cases. Particle rotation is calculated as the angular velocity in radians/sec. Multiple soft particles from different parts of the sample are tracked. It is observed that the rotational velocity gradually reduces with compression in both cases, and the magnitude of particle rotation for both cases is nearly similar (Fig. 10) at a higher compression level (>200 kPa).



**Figure 10.** Particle spin analysis with increasing compression.

Rolling friction is found to be an essential factor for simulating soft-rigid sample response to some extent. However, such an effect is insignificant beyond a certain magnitude of rolling friction. In addition, varying rolling friction is also found ineffective. This observation may happen because, in 1-D compression, particle rotation is limited, unlike other shear-induced loading scenarios. The mixture response with the proposed calibration, especially for higher soft particle content, indicates a qualitative agreement between the experimental and numerical results. The results can be further improved by utilizing non-linear contact stiffness and rolling friction.

#### 4. Conclusions and future scope

It is evident from the CT-scan images that the soft particles deform significantly under compressive loading. This changes the contact properties between soft-soft, and soft-rigid contacts. The DEM simulation presented here indicates that rolling resistance is a simple way to consider the shape of the granular particles in DEM. The adopted contact model better predicts the behaviour of these unconventional mixtures than the simple linear contact models with sliding friction alone. However, results indicate that rolling friction can improve the prediction only to a certain extent. In order to enhance the evolving contact stiffness of soft particles, a more sophisticated contact model along with rolling friction is necessary. Hence, the numerical and experimental observations agree with the lower soft particle content sample in the present analysis. Detailed shapes must be performed for the higher soft content samples to better match the experimental and numerical results. For the future scope of the study, two ways to predict the behaviour of such mixtures are recommended. 1) to find a direct correlation between particle shape and rolling friction and 2) using real-shaped particles from CT scan images and preparing soft particles as flexible.

#### Acknowledgments

The authors would like to thank Melbourne TrACEES (Trace Analysis for Chemical, Earth and Environmental Sciences) platform for access to the micro-CT scanner and Dr. Jay Black for technical support.

#### References

- Ahmadi, M., Madadi, M., Disfani, M., Shire, T., & Narsilio, G. "Reconstructing the microstructure of real gap-graded soils in DEM: Application to internal instability". *Powder Technology*, 394, 504–522, 2021. <https://doi.org/10.1016/J.POWTEC.2021.08.073>
- Asadi, M., Mahboubi, A., & Thoeni, K. "Discrete modeling of sand–tire mixture considering grain-scale deformability". *Granular Matter*, 20(2), 18, 2018. <https://doi.org/10.1007/s10035-018-0791-4>
- Asadi, M., Thoeni, K., & Mahboubi, A. "An experimental and numerical study on the compressive behavior of sand-rubber particle mixtures". *Computers and Geotechnics*, 104, 185–195, 2018. <https://doi.org/10.1016/j.compgeo.2018.08.006>
- Fonseca, J., Riaz, A., Bernal-Sanchez, J., Barreto, D., McDougall, J., Miranda-Manzanares, M., Marinelli, A., & Dimitriadi, V. "Particle-scale interactions and energy dissipation mechanisms in sand-rubber mixtures". *Geotechnique Letters*, 9(4), 263–268, 2019. <https://doi.org/10.1680/jgele.18.00221>
- Gong, L., Nie, L., Xu, Y., Wang, H., Zhang, T., Du, C., & Wang, Y. "Discrete element modelling of the mechanical behaviour of a sand-rubber mixture containing large rubber particles". *Construction and Building Materials*, 205, 574–585, 2019. <https://doi.org/10.1016/J.CONBUILDMAT.2019.01.214>
- Kim, H. K., & Santamarina, J. C. "Sand-rubber mixtures (large rubber chips)". *Canadian Geotechnical Journal*, 45(10), 1457–1466, 2008. <https://doi.org/10.1139/T08-070>
- Lee, C., Truong, ; Q Hung, Lee, W., & Lee, J.-S. "Characteristics of Rubber-Sand Particle Mixtures according to Size Ratio". *Journal of Materials in Civil Engineering*, 22(4), 323–331, 2009. [https://doi.org/10.1061/\(ASCE\)MT.1943-5533.0000027](https://doi.org/10.1061/(ASCE)MT.1943-5533.0000027)
- Lee, J. H., Salgado, R., Bernal, A., & Lovell, C. W. "Shredded Tires and Rubber-Sand as Lightweight Backfill". *Journal of Geotechnical and Geoenvironmental Engineering*, 125(2), 132–141, 1999. [https://doi.org/10.1061/\(asce\)1090-0241\(1999\)125:2\(132\)](https://doi.org/10.1061/(asce)1090-0241(1999)125:2(132))
- Lee, J.-S., Dodds, J., & Santamarina, J. C. "Behavior of Rigid-Soft Particle Mixtures. *Journal of Materials in Civil Engineering*", 19(2), 179–184, 2007. [https://doi.org/10.1061/\(ASCE\)0899-1561\(2007\)19:2\(179\)](https://doi.org/10.1061/(ASCE)0899-1561(2007)19:2(179))
- Liu, X., Tian, C., & Lan, H. "Laboratory investigation of the mechanical properties of a rubber-calcareous sand mixture: The effect of rubber content". *Applied Sciences (Switzerland)*, 10(18), 6583, 2020. <https://doi.org/10.3390/APP10186583>
- Liu, Y., Liao, X., Li, L., & Mao, H. "Discrete element modelling of the mechanical behavior of sand–rubber mixtures under true triaxial tests". *Materials*, 13(24), 1–24, 2020. <https://doi.org/10.3390/ma13245716>
- Lopera Perez, J. C., Kwok, C. Y., & Senetakis, K. "Effect of rubber size on the behaviour of sand-rubber mixtures: A numerical investigation". *Computers and Geotechnics*, 80, 199–214, 2016. <https://doi.org/10.1016/J.COMPGEO.2016.07.005>
- Ma, K., Wang, L., Long, L., Peng, Y., & He, G. "Discrete element analysis of structural characteristics of stepped reinforced soil retaining wall". *Geomatics, Natural Hazards and Risk*, 11(1), 1447–1465, 2020. <https://doi.org/10.1080/19475705.2020.1797907>
- Wang, C., Deng, A., & Taheri, A. "Three-dimensional discrete element modeling of direct shear test for granular rubber–sand". *Computers and Geotechnics*, 97, 204–216, 2018. <https://doi.org/10.1016/J.COMPGEO.2018.01.014>